Journal of Power Sources 260 (2014) 77–81

Contents lists available at ScienceDirect

Journal of Power Sources

journal homepage: www.elsevier.com/locate/jpowsour

Short communication

Nickel- and platinum-containing core@shell catalysts for hydrogen generation of aqueous hydrazine borane

D. Clémençon [a], J.F. Petit [a], U.B. Demirci [a,*], Q. Xu [b], P. Miele [a]

[a] IEM (Institut Europeen des Membranes), UMR 5635 (CNRS-ENSCM-UM2), Universite Montpellier 2, Place E. Bataillon, F-34095 Montpellier, France
[b] National Institute of Advanced Industrial Science and Technology (AIST), Ikeda, Osaka 563-8577, Japan

HIGHLIGHTS

- Nickel and platinum were used to prepare a series of core@shell nano-structures.
- The core@shell nano-structures were used for catalytic dehydrogenation of $N_2H_4BH_3$.
- Ni_5@Pt permitted to generate 4.5 mol $H_2 + N_2$ per mol $N_2H_4BH_3$ at 50 °C.
- The efficiency of Ni_5@Pt is due to the presence of both metals on the surface.
- The core@shell nano-catalysts have accordingly the structure Ni@NiPt.

GRAPHICAL ABSTRACT

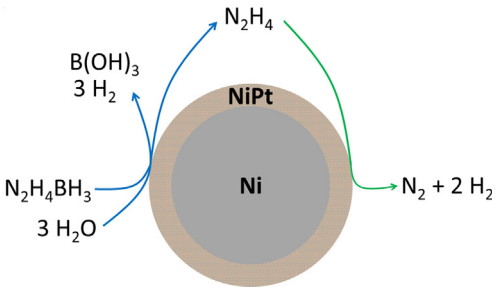

ARTICLE INFO

Article history:
Received 11 December 2013
Received in revised form
27 February 2014
Accepted 5 March 2014
Available online 16 March 2014

Keywords:
Core@shell nano-structures
Hydrazine borane
Hydrolysis
Nickel
Platinum

ABSTRACT

Nickel and platinum were used to prepare a series of core@shell structures to be studied as catalysts for the dehydrogenation of aqueous hydrazine borane $N_2H_4BH_3$ at 50 °C. The challenge was especially to get a maximum of 3 mol of gas by decomposition of the N_2H_4 moiety. In our conditions, the most efficient Ni@Pt was found to be the structure constituted of 5 atoms of nickel for 1 atom of platinum. This catalyst permits to generate up to 4.5 mol $H_2 + N_2$. Surface characterizations showed that the efficiency of this catalyst is due to the presence of both metals on the surface, suggesting therefore that the structure would be rather Ni@NiPt. Our main results are reported herein.

1. Introduction

Hydrazine borane $N_2H_4BH_3$ (HB) has been recently presented as a promising hydrogen storage material. Hügle et al. [1] showed that an equimolar mixture of HB and lithium hydride is able to show an effective gravimetric storage capacity of 11 wt% H_2 when kept at 150 °C for 1 h. Pristine HB is however not suitable because of the release of significant amounts of hydrazine and formation of a shock-sensitive solid residue upon prolonged heating [2,3]. For thermolytic dehydrogenation, it is preferable to use derivatives of HB, *i.e.* lithium or sodium hydrazinidoborane $MN_2H_3BH_3$ (M = Li or Na), obtained by ball-milling the borane with the alkaline hydride [4,5].

Another way of dehydrogenating HB is hydrolysis (Eq. (1)). Half of H_2 is provided by water but only the BH_3 group is dehydrogenated [6,7]. Recently, we have demonstrated that the decomposition of the N_2H_4 moiety could be achieved in the presence of a

* Corresponding author. Tel.: +33 (0)4 67 14 91 60; fax: +33 (0)4 67 14 91 19.
E-mail address: umit.demirci@um2.fr (U.B. Demirci).

http://dx.doi.org/10.1016/j.jpowsour.2014.03.015
0378-7753/

suitable nickel-based bimetallic catalyst [8]. The decomposition can follow 2 different paths (Eqs. (2) and (3)) and the challenge is to favor the dehydrogenation reaction (Eq. (3)). Nickel–platinum or nickel–rhodium nano-particles (alloys) are good candidates in that, but the selectivity in H_2 is not of 100% yet [9,10]. This is illustrated by Eq. (4) where x represents the fraction of N_2H_4 leading to $H_2 + N_2$. With the ideal catalyst, it is expected the formation of 5 mol of H_2 and 1 mol of N_2 per mole of HB (Eq. (5)).

$$N_2H_4BH_3 + 3H_2O \rightarrow N_2H_4 + B(OH)_3 + 3H_2 \quad (1)$$

$$N_2H_4 \rightarrow 4/3NH_3 + 1/3N_2 \quad (2)$$

$$N_2H_4 \rightarrow N_2 + 2H_2 \quad (3)$$

$$N_2H_4BH_3 + 3H_2O \rightarrow (1+2x)/3N_2 + 4(1-x)/3NH_3 + B(OH)_3 + (3+2x)H_2 \quad (4)$$

$$N_2H_4BH_3 + 3H_2O \rightarrow N_2 + B(OH)_3 + 5H_2 \quad (5)$$

Catalyzed dehydrogenation of N_2H_4 of HB faces several issues and the 3 main challenges touch the catalyst. It has to be (*i*) active, (*ii*) 100%-selective and (*iii*) stable. Accordingly, efforts have been dedicated to find (*i*) active and (*ii*) selective catalysts. This is illustrated in the present work where core@shell nano-structures were prepared to be used as catalysts for dehydrogenation of HB.

2. Material and methods

A series of Ni_α@Pt nano-particles (α = 4, 5, 7, 10, 40, with α defined as: α moles of Ni for 1 mol of Pt) were prepared according to a modified version of the method reported in Ref. [11]. Under argon, a mass of nickel acetylacetonate ($Ni(C_5H_7O_2)_2$, Strem-Chemicals), 1170 mg of potassium hydroxide (KOH, Sigma–Aldrich) and 520 mg of hexadecyltrimethylammonium bromide (CTAB, $CH_3(CH_2)_{15}N(Br)(CH_3)_3$, Sigma–Aldrich) were transferred in a Schlenk balloon. 1,2-propanediol ($C_3H_8O_2$, Sigma–Aldrich, 60 mL) was added. The slurry was stirred to dissolve the solids. This solution (S1) was heated at 120 °C for 30 min. In the meantime, a hydrazine ($N_2H_4{\cdot}H_2O$, Sigma–Aldrich, 3.6 mL) solution (S2) of sodium borohydride ($NaBH_4$, Acros Organics, 156 mg) was prepared. The heater was turned off before the addition of S2 into S1. The green color of S1 turned black by reduction of Ni^{2+}. The resulting solution (S3) was ultrasonicated for 15 min and heated. At 120 °C, a mass of sodium hexachloroplatinate hexahydrate ($Na_2PtCl_6{\cdot}6H_2O$, Sigma–Aldrich) in 1,2-propanediol was added into S3, to deposit Pt by galvanic replacement. The nano-particles were recovered by centrifugation, washed with water and ethanol several times, and dried at 65 °C overnight. For every preparation, 43 mg of catalyst were synthesized. Pure nickel nano-particles were also prepared.

Characterization was performed by powder X-ray diffraction (XRD, Bruker D5005, CuKα radiation, λ = 1.5406 Å), scanning-electron microscopy (SEM, Hitachi S4800), energy-dispersive X-ray spectroscopy (EDX, Thermofisher 6213 detector), transmission-electron microscopy (TEM, JEOL 1200 EXII) and X-ray photoelectron spectroscopy (XPS, Thermo Electron ESCALAB 250, Al Kα, $h\nu$ = 1486.6 eV; calibration using the position of C 1s core level 284.8 eV).

A fresh aqueous solution of HB (42.5 mg in 1.5 mL H_2O) was prepared for every dehydrogenation experiments. Millipore milli-q water (resistivity > 18 MΩ cm) was used. The experimental details are given in the caption of each figure. Detailed procedures for the HB synthesis and the dehydrogenation experiments were described previously [3,8]. Typically, in an argon-filled glove box, the catalyst is introduced into a 100 mL round-bottom flask. The glassware is placed in a water bath at 50 °C and connected to a water-filled inverted burette. Should some NH_3 evolve, a trap filled with a 0.01 M HCl aqueous solution is placed between the flask and a cold trap at 0 °C. Then, the HB solution is injected and the gas evolution video-recorded, to be later exploited by using the soft Matlab. Each catalyst was tested at least twice to ensure results reproducibility (maximized error bars are given where informative).

3. Results and discussion

The presence of both metals was verified by EDX [12]. The formation of the shell was tentatively scrutinized by SEM. Three samples were selected (Ni, Ni_{40}@Pt, Ni_5@Pt) and compared. The interpretation of the images was realized with the help of the reference [13]. Pu et al. showed that the formation of a gold shell on $BaTiO_3$ particles implies adsorption of 2–3 nm gold nano-particles on the surface of the core, and then formation of the complete gold shell through seeded condensation. The SEM images of our samples are shown in Fig. 1. The Ni particles (60–80 nm) are agglomerated into large aggregates, which surface is almost smooth. The surface of nickel changes with the addition of platinum, becoming rougher. The images were compared to those in the reference [13]: it stood out evident resemblances between Ni_α@Pt and $BaTiO_3$@Au.

Nickel and platinum are effective catalysts in hydrolysis of B–H bonds [14]. However, in our conditions, the nickel nano-particles are not able to generate 3 mol of H_2 by hydrolysis of BH_3 (Fig. 2a). Only 2.2 mol of gas evolved, with the hydrogen generation rate (HGR) being 4.5 mL min^{-1}. Furthermore, the addition of a small amount of Pt does not significantly improve the catalytic activity as Ni_{40}@Pt catalyzes the evolution of 2.4 mol of gas only, suggesting incomplete hydrolysis of BH_3. Nevertheless, the HGR is improved with 73.5 mL min^{-1} (4.3 L min^{-1} g). The presence of residual BH_3 in both cases was verified by ^{11}B NMR [15]. The reason of such low

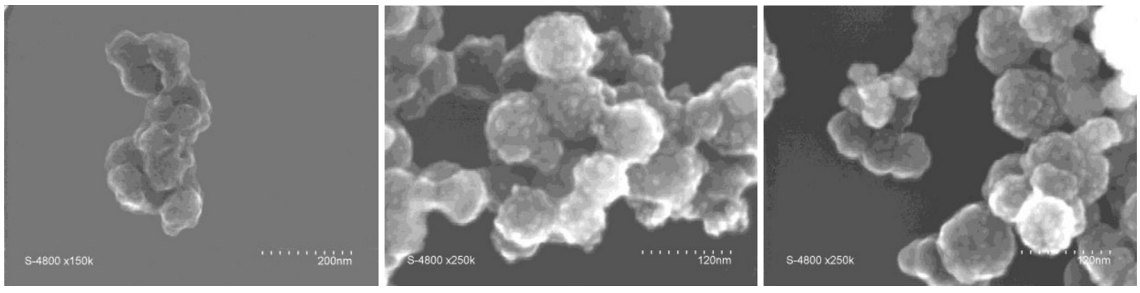

Fig. 1. SEM images of Ni (left), Ni_{40}@Pt (middle) and Ni_5@Pt (right).

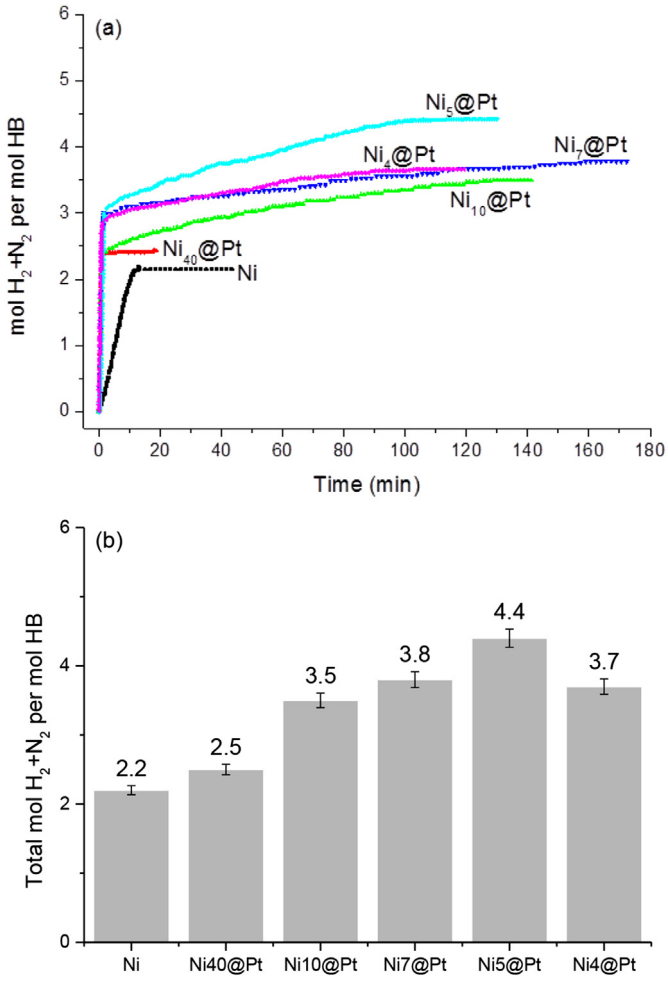

Fig. 2. (a) Time evolution of $H_2 + N_2$ for the dehydrogenation of HB in the presence of Ni or Ni_α@Pt at 50 °C, and (b) evolution of the total mole number of $H_2 + N_2$ as a function of Ni_α@Pt (error bar ± 3%). The dehydrogenation experiments were performed at 50 °C, using 17 mg of catalyst and a fresh solution of HB (42.5 mg in 1.5 mL H_2O).

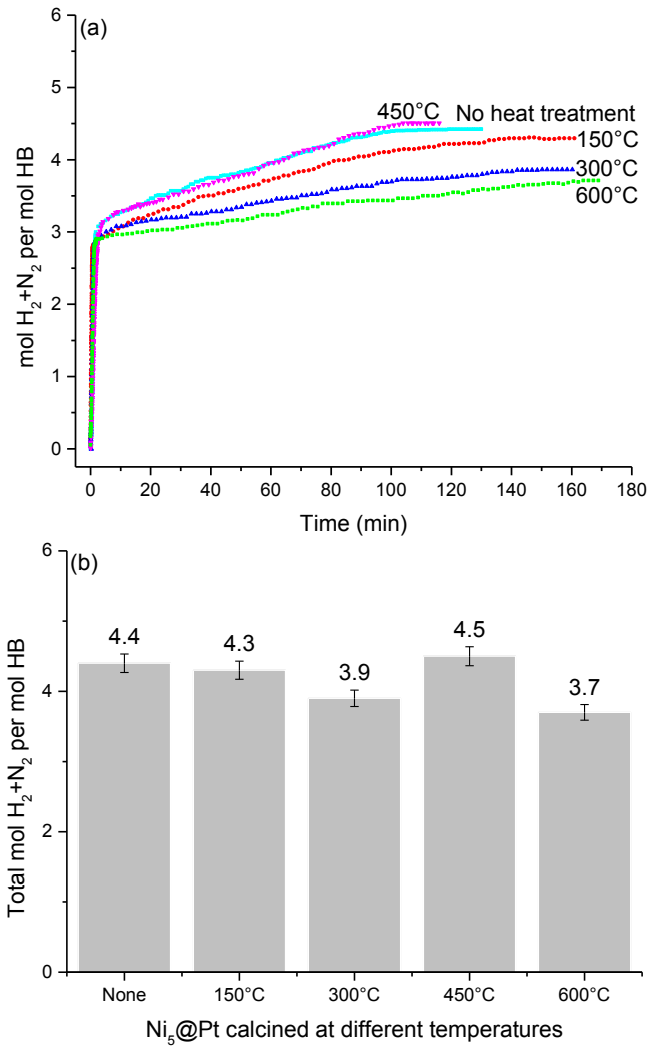

Fig. 3. (a) Time evolution of $H_2 + N_2$ for the dehydrogenation of HB at 50 °C in the presence of Ni_5@Pt and Ni_5@Pt heat-treated at different temperatures (150, 300, 450 and 600 °C), and (b) evolution of the total mole number of $H_2 + N_2$ (error bar ± 3%) as a function of the temperature of heat treatment. The dehydrogenation experiments were performed at 50 °C, using 17 mg of catalyst and a fresh solution of HB (42.5 mg in 1.5 mL H_2O).

activity is not fully understood yet; surface passivation by strong adsorption of borates and/or oxidation could be suggested.

With higher Pt loadings, Ni_α@Pt is able to generate more than 3 mol of gas per mole of HB (Fig. 2a). They are capable to hydrolyze the BH_3 groups and in addition show activity in the decomposition of the N_2H_4 moiety. The decomposition of HB in the presence of Ni_{10}@Pt, Ni_7@Pt, Ni_5@Pt and Ni_4@Pt is characterized by 2 steps. The first one, mainly due to hydrolysis of BH_3, shows fast kinetics of H_2 generation. The HGRs are within the range 70–75 mL min^{-1} (4.1–4.4 L min^{-1} g). The second step attributed to the decomposition of N_2H_4 shows much lower kinetics of $H_2 + N_2$ formation (NH_3 is not taken into account as it is trapped before measurement). The HGRs are <0.2 mL min^{-1} (<13 mL min^{-1} g). Note that decomposition of N_2H_4 also takes place during the first step but because of slow kinetics its occurrence is negligible [16].

The variation of the mole number of $H_2 + N_2$ as a function of the nickel content in Ni_α@Pt is shown in Fig. 2b. It has a volcano shape and the maximum peak is observed for Ni_5@Pt. As reported elsewhere, electronic and/or geometric effects could rationalize such reactivity changes [17], which is in fact the searched effect when 2 metals are combined as alloy or core@shell. To sum up, our core@shell catalysts overcome the challenge (*i*), namely there are active in decomposition of N_2H_4 of HB.

Better selectivity in H_2 could be achieved with a surface composed of both metals. As the Ni_α@Pt nano-particles are presumably made of a core of nickel and a shell of platinum, annealing was envisaged to activate the segregation of nickel. The occurrence of such segregation can be predicted from the sublimation enthalpy of each metal [18] and from theoretical results obtained by DFT calculations [19]. Accordingly, the best catalyst Ni_5@Pt was annealed and the following conditions were applied: 150, 300, 450 or 600 °C; 5 °C min^{-1}; 4 h; argon flow. The results are reported in Fig. 3. Annealing at 150 °C has almost no effect on the activity of Ni_5@Pt while that at 300 °C is detrimental with a mole number of $H_2 + N_2$ decreasing to 3.9. This could be explained by a surface evolution as TEM observations did not show obvious aggregation of the nano-particles and/or obvious growth of the aggregated particles (Fig. 4). With a further increase of the annealing temperature to 450 °C, the activity of Ni_5@Pt improves. A mole number of $H_2 + N_2$ of 4.5 was found. This could be the consequence of nickel segregation and combination (possibly, alloying) of both metals at the surface of the nano-particles. At higher annealing temperature, the mole number of $H_2 + N_2$ decreases. This could be due to an

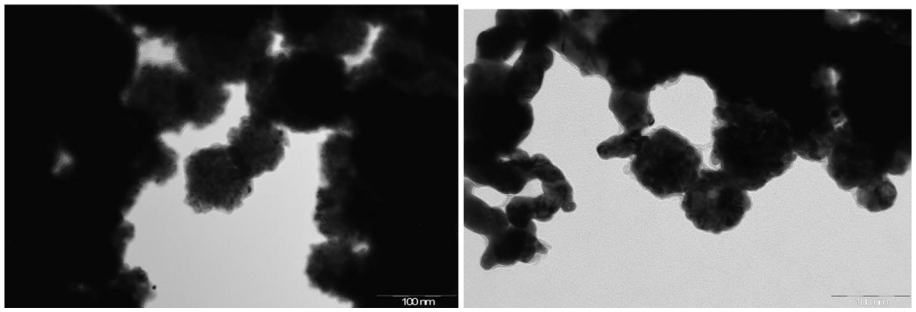

Fig. 4. TEM images of Ni_5@Pt (left) and Ni_5@Pt (right) annealed at 450 °C.

aggregation of the particles and/or a surface modification. With respect to the HGRs, they are within the range 70–75 mL min^{-1} (4.1–4.4 L min^{-1} g) for the hydrolysis of BH_3, independently on the nano-particles. For the decomposition of N_2H_4, there is an effect of the temperature of the heat treatment on the HGRs: one can see a slight deviation of the curves slopes for this reaction.

Characterization by powder XRD was performed on both Ni_5@Pt and the sample annealed at 450 °C. For comparison, the nano-particles annealed at the other temperatures were also analyzed (Fig. 5). The pattern of Ni_5@Pt shows 5 diffraction peaks, ascribed to platinum (ICDD 00-004-0802). This result suggests that the nickel compound would be amorphous. A similar pattern is observed for Ni_5@Pt annealed at 150 °C. From 300 °C, the crystalline state of the nano-particles evolves. In addition to the diffraction peaks of platinum, there are 3 peaks ascribed to nickel (ICDD 03-065-2865). The change is more important after annealing at 450 °C. In addition to the peaks of nickel, peaks ascribed to nickel oxide (ICDD 01-075-0269) are found. With respect to platinum (ICDD 01-087-0687), the peaks have broadened and shifted to higher angles (shift of ~0.5°). For the sample heated up to 600 °C, nickel (ICDD 03-065-2865) and platinum (ICDD 01-087-0687) have been detected. There are additional small diffraction peaks which identification has not been easy. They might be ascribed to a nickel–platinum alloy (ICDD 03-065-2797).

The surface state of Ni_5@Pt before and after annealing at 450 °C was analyzed by XPS. Both metals were detected within the analyzed layer of 3 nm, suggesting that the shell thickness is lower than 3 nm or that both metals are present on the surface. The spectra are shown in Fig. 6. They were analyzed with the help of available database [20]. Annealing has no significant effect on the oxidation state of nickel as the spectra are very similar. The signals are easily ascribed to Ni(II). There is nevertheless a slight difference. One can observe a shift of few tens of eV towards the high binding energies (BEs), which may be explained by a slightly increased

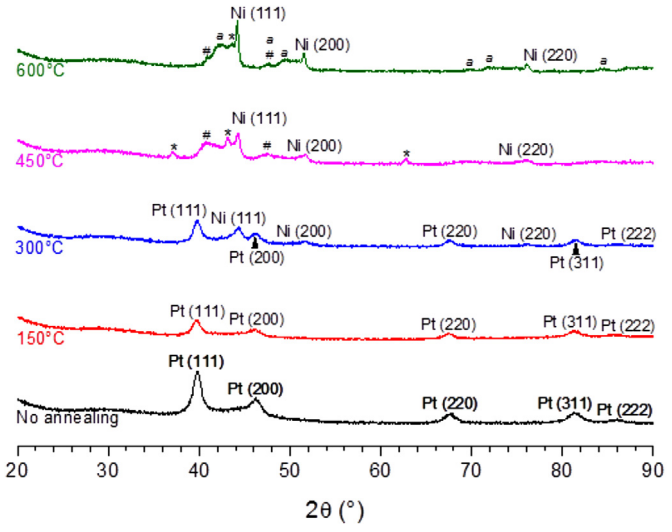

Fig. 5. XRD patterns of Ni_5@Pt and Ni_5@Pt heat-treated at different temperatures (150, 300, 450 and 600 °C). The signs *, # and a points the peaks ascribed to NiO, Pt, and Ni–Pt alloy respectively.

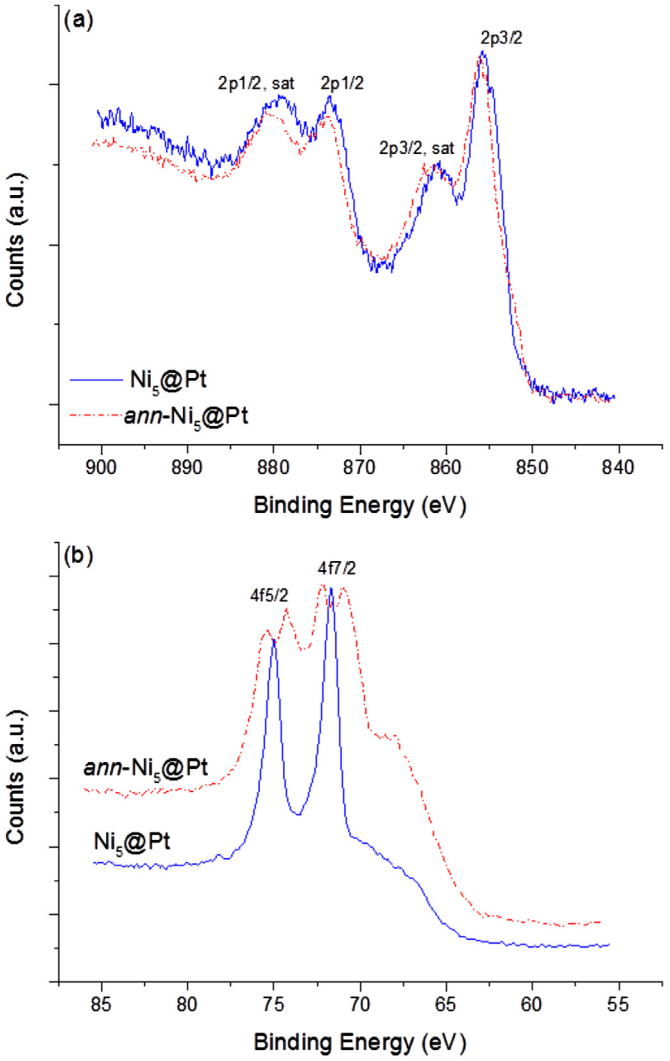

Fig. 6. XPS spectra of Ni_5@Pt and Ni_5@Pt annealed at 450 °C (denoted *ann*-Ni_5@Pt): (a) spectra for Ni 2p and (b) spectra for Pt 4f.

oxidation. With respect to platinum in Ni_5@Pt, the BE of Pt 4f7/2 (71.7 eV) may be attributed to platinum in an alloy or in a salt. This is confirmed by the BE of Pt 4f5/2. Annealing has an effect on the platinum surface state. The presence of metallic platinum (70.9 eV for Pt 4f7/2) is found but there is a slight increase of the oxidation of some other platinum (72.3 eV for Pt 4f7/2). The XPS analysis also permitted a semi-quantitative analysis of both metals. These BE values are suggestive of the formation/presence of some NiPt alloy as well as the presence of both metals deposited separately. For Ni_5@Pt, it was found a molar ratio Ni:Pt of 1.9:1. The ratio is lower than the experimental target 5:1 because the XPS analysis is done for a layer of 3 nm. For annealed Ni_5@Pt, the ratio has increased to 2.8:1, suggesting a surface segregation of nickel. Consequently, the better results obtained after annealing at 450 °C may be ascribed to the presence of both metals at the surface.

Our results show that a core@shell structure based on nickel and platinum is able to decompose the N_2H_4 moiety of HB after hydrolysis of the BH_3 group. However, to favor the dehydrogenation of N_2H_4, the presence of both metals in the shell and thus on the particle surface is crucial.

4. Conclusions

Effective dehydrogenation of hydrazine borane is dependent on the ability of the catalyst to hydrolyze the BH_3 group of the borane and also to dehydrogenate the N_2H_4 group while avoiding its decomposition into NH_3. For this purpose, we have developed in the present work, and for the first time, a series of core@shell structures where the core and the shell are made of nickel and platinum respectively. Most of the structures are catalytically active in the hydrolysis of BH_3 and the decomposition on N_2H_4. With the sample Ni_5@Pt annealed at 450 °C, up to 4.5 mol of $H_2 + N_2$ can be generated at 50 °C. The performed characterizations suggest that the efficiency of the catalyst is dependent on the presence of both metals in the shell, *i.e.* on the surface. In other words, the best results are obtained with Ni_5@Pt annealed at 450 °C, which structure is in fact assumed to be Ni@NiPt. Better performance could be achieved *via* optimization of the nano-particles size as well as of the surface composition.

References

[1] T. Hügle, M.F. Kühnel, D. Lentz, J. Am. Chem. Soc. 131 (2009) 7444–7446.
[2] J. Goubeau, E. Ricker, Z. Anorg. Allg. Chem. 310 (1961) 123–142.
[3] R. Moury, G. Moussa, U.B. Demirci, J. Hannauer, S. Bernard, E. Petit, A. van der Lee, P. Miele, Phys. Chem. Chem. Phys. 14 (2012) 1768–1777.
[4] H. Wu, W. Zhou, F.E. Pinkerton, T.J. Udovic, T. Yildirim, J.J. Rush, Energy Environ. Sci. 5 (2012) 7531–7535.
[5] R. Moury, U.B. Demirci, T. Ichikawa, Y. Filinchuk, R. Chiriac, A. van der Lee, P. Miele, ChemSusChem 6 (2013) 667–673.
[6] S. Karahan, M. Zahmakiran, S. Özkar, Int. J. Hydrogen Energy 36 (2011) 4958–4966.
[7] D. Çelik, S. Karahan, M. Zahmakiran, S. Özkar, Int. J. Hydrogen Energy 37 (2012) 5143–5151.
[8] Ç. Çakanyıldırım, U.B. Demirci, T. Şener, Q. Xu, P. Miele, Int. J. Hydrogen Energy 37 (2012) 9722–9729.
[9] J. Hannauer, O. Akdim, U.B. Demirci, C. Geantet, J.M. Herrmann, P. Miele, Q. Xu, Energy Environ. Sci. 4 (2011) 3355–3358.
[10] D.C. Zhong, K. Aranishi, A.K. Singh, U.B. Demirci, Q. Xu, Chem. Commun. 48 (2012) 11945–11947.
[11] G. Wang, H. Wu, D. Wexler, H. Liu, O. Savadogo, J. Alloys Compd. 503 (2010) L1–L4.
[12] For brevity, the EDX spectra are not reported herein.
[13] Y. Pu, R. Grange, C.L. Hsieh, D. Psaltis, Phys. Rev. Lett. 104 (2010), 207402:1–4.
[14] M. Yadav, Q. Xu, Energy Environ. Sci. 5 (2012) 9698–9725.
[15] For brevity, the NMR (solution-state ^{11}B) spectra are not reported herein. For Ni and Ni40@Pt, the presence of residual BH_3 was observed after analysis of the spent fuel by NMR (quartet at around −20 ppm). For the other Ni_α@Pt, a broad singlet was observed at around 9 ppm (borate by-products). For more details about similar NMR results, please refer to Refs. [16,17].
[16] Ç. Çakanyıldırım, E. Petit, U.B. Demirci, R. Moury, J.F. Petit, Q. Xu, U.B. Demirci, Int. J. Hydrogen Energy 37 (2012) 15983–15991.
[17] J. Hannauer, U.B. Demirci, C. Geantet, J.M. Herrmann, P. Miele, Int. J. Hydrogen Energy 37 (2012) 10758–10767.
[18] M.P. Seah, J. Catal. 57 (1979) 450–457.
[19] B. Hammer, J.K. Nørskov, Adv. Catal. 45 (2000) 71–129.
[20] NIST X-ray Photoelectron Spectroscopy Database, available at: http://srdata.nist.gov/xps/, consulted in November 2013.